Antimicrobial Agents and Chemotherapy

The Second Extracellular Loop of CCR5 Contains the Dominant Epitopes for Highly Potent Anti-Human Immunodeficiency Virus Monoclonal Antibodies

Jun Zhang, Eileen Rao, Marianna Dioszegi, Rama Kondru, Andre DeRosier, Eva Chan, Stephan Schwoerer, Nick Cammack, Michael Brandt, Surya Sankuratri and Changhua Ji

Antimicrob. Agents Chemother. **2007, 51(4):1386. DOI: 10.1128/AAC.01302-06.**
Published Ahead of Print 22 January 2007.

ANTIMICROBIAL AGENTS AND CHEMOTHERAPY, Apr. 2007, p. 1386–1397 Vol. 51, No. 4
0066-4804/07/$08.00+0 doi:10.1128/AAC.01302-06

The Second Extracellular Loop of CCR5 Contains the Dominant Epitopes for Highly Potent Anti-Human Immunodeficiency Virus Monoclonal Antibodies▽

Jun Zhang,[1] Eileen Rao,[1] Marianna Dioszegi,[1] Rama Kondru,[2] Andre DeRosier,[1] Eva Chan,[1] Stephan Schwoerer,[3] Nick Cammack,[1] Michael Brandt,[3] Surya Sankuratri,[1] and Changhua Ji[1]*

Viral Diseases[1] and Chemistry,[2] Roche Palo Alto, Palo Alto, California 94304, and Pharmaceuticals Division, Roche Penzberg, Penzberg, Germany[3]

Received 18 October 2006/Returned for modification 27 December 2006/Accepted 12 January 2007

Six mouse anti-human CCR5 monoclonal antibodies (mAbs) that showed potent antiviral activities were identified from over 26,000 mouse hybridomas. The epitopes for these mAbs were determined by using various CCR5 mutants, including CCR5/CCR2B chimeras. One mAb, ROAb13, was found to bind to a linear epitope in the N terminus of CCR5. Strikingly, the other five mAbs bind to epitopes derived from extracellular loop 2 (ECL2). The three most potent mAbs, ROAb12, ROAb14, and ROAb18, require residues from both the N-terminal (Lys171 and Glu172) and C-terminal (Trp190) halves of ECL2 for binding; two other mAbs, ROAb10 and ROAb51, which also showed potent antiviral activities, require Lys171 and Glu172 but not Trp190 for binding. Binding of the control mAb 2D7 completely relies on Lys171 and Glu172. Unlike 2D7, the novel mAbs ROAb12, ROAb14, and ROAb18 do not bind to the linear peptide 2D7-2SK. In addition, all three mAbs bind to monkey CCR5 (with Arg at position 171 instead of Lys); however, 2D7 does not. Since five of the six most potent CCR5 mAbs derived from the same pool of immunized mice require ECL2 as epitopes, we hypothesize that CCR5 ECL2 contains the dominant epitopes for mAbs with potent antiviral activities. These dominant epitopes were found in CCR5 from multiple species and were detected in large proportions of the total cell surface CCR5. mAbs recognizing these epitopes also showed high binding affinity. A homology model of CCR5 was generated to aid in the interpretation of these dominant epitopes in ECL2.

C-C chemokine receptor CCR5 belongs to family A of G-protein-coupled receptors with the characteristic seven transmembrane domains. CCR5 is responsible for leukocyte trafficking to sites of inflammation in response to its natural ligands RANTES (regulated on activation, normal T-cell expressed and secreted), macrophage inhibitory protein 1α, and macrophage inhibitory protein 1β. CCR5 was also found to be the primary coreceptor for human immunodeficiency virus (HIV) (11, 12). HIV enters the host cell via the interaction of the viral envelope (Env) protein gp160 and host cell membrane proteins. Synthesized as a single polypeptide precursor, Env is subsequently cleaved by a cellular protease to generate two noncovalently associated subunits, gp120 and gp41. gp120 binds to the cell surface, whereas the membrane-spanning gp41 subunit mediates membrane fusion. The primary receptor for HIV type 1 (HIV-1) is CD4. Binding of gp120 to CD4 results in multiple conformational changes in gp120, which is required for the interaction between gp120 and coreceptors. Binding of gp120 to the coreceptor triggers structural changes within gp41 that lead to virus-host cell fusion.

There are two main coreceptors for HIV, CCR5 and CXCR4 (11, 12, 16). The majority of primary HIV-1 strains use CCR5 as a coreceptor (termed R5 virus), whereas some viruses are able to use another chemokine receptor, CXCR4, as a coreceptor (termed X4 virus) or use both CCR5 and CXCR4 as coreceptors (termed R5X4 virus). CCR5 plays a pivotal role in HIV transmission and pathogenesis. R5 viruses were found in a majority of primary infections, and they usually persist during the entire course of infection. It has been observed that genetically CCR5-deficient (Δ32) individuals are essentially protected against infection by HIV-1 in high-risk populations (26, 37), and heterozygous Δ32 individuals are often long-term nonprogressors (14). Therefore, CCR5 has become a very attractive target for the development of novel anti-HIV drugs. A number of small-molecule CCR5 antagonists or monoclonal antibodies (mAbs) that demonstrated potent antiviral effects both in cell culture and in clinical trials have been identified (24, 27, 39, 41, 42).

CCR5 contains four extracellular domains: the N terminus (Nt), extracellular loop 1 (ECL1), ECL2, and ECL3. Due to the lack of a well-defined three-dimensional structure of CCR5, an understanding of the functional domains of CCR5 has proven to be difficult. Most of the information on the CCR5 domains involved in the interaction with HIV gp120 was obtained from studies using mutated and chimeric molecules. Despite the complexity of the picture, it is believed that the Nt plays a critical role in CCR5-gp120 interactions. The Nt of CCR5 is posttranslationally modified by the addition of sulfate moieties to tyrosine residues at positions 3, 10, 14, and 15. The sulfation of these tyrosines, particularly at positions 3 and 10, has been shown to facilitate HIV entry (15), possibly through enhanced electrostatic interactions with positively charged amino acids in the bridging sheet and the V3 base (2). Although the CCR5 N terminus itself, when transplanted onto another chemokine receptor, CCR1, is sufficient for mediating

* Corresponding author. Mailing address: Roche Palo Alto, 3431 Hillview Avenue, Palo Alto, CA 94304. Phone: (650) 855-6429. Fax: (650) 852-1350. E-mail: Changhua.ji@roche.com.

▽ Published ahead of print on 22 January 2007.

viral entry, the affinity of soluble gp120-CD4 for CCR5 Nt sulfopeptides is 10- to 100-fold lower than that for native CCR5. This finding suggests that another exodomain(s) of CCR5 is also involved in gp120-CCR5 interactions. In fact, it has been suggested that gp120 docking to CCR5 is a multistep process involving several independent regions of gp120 and CCR5 (9, 13, 33). In addition to the Nt, ECL2 is believed to be involved in HIV entry, possibly by making contact with the tip of the gp120 V3 loop (8, 34).

Although a number of CCR5 mAbs have been described, few of them have demonstrated potent antiviral activities. Epitope mapping revealed that these mAbs recognize a variety of different epitopes that can be roughly classified into three categories: Nt, ECL2, and multidomain (25). Previously published results suggest that Nt-binding mAbs inhibit gp120 binding effectively, yet they inhibit HIV fusion only moderately. In contrast, ECL2-binding mAbs inhibit HIV fusion potently, but they inhibit gp120 binding only moderately (25, 30). Three CCR5 mAbs, 2D7, PRO 140, and mAb004, that showed potent antiviral activities are currently in development as potential inhibitors of HIV entry.

In the current study, we screened more than 26,400 hybridoma lines for mAbs that bind to CCR5 and inhibit HIV fusion/entry. About 400 lines of hybridomas were found to produce mAbs with CCR5-binding activity. These mAbs were further tested for HIV fusion inhibition, seven clones were further characterized, and six of them were found to be potent HIV entry inhibitors. The four most potent mAbs were fully characterized in various functional assays (20). Here, we report the epitope mapping data for these six mAbs. Out of the four most potent mAbs (in peripheral blood mononuclear cell [PBMC] antiviral assays), three bind to similar epitopes derived from ECL2. Furthermore, two other mAbs with potency equal to or greater than that of 2D7 were also found to use epitopes derived from ECL2. Therefore, five out of the six most potent CCR5 mAbs derived from over 26,000 hybridomas bind to ECL2. These data demonstrate that CCR5 ECL2 contains the dominant epitopes for mAbs with highly potent antiviral activities.

MATERIALS AND METHODS

Reagents. All cell culture media and supplements and fetal bovine serum were purchased from Invitrogen (Carlsbad, CA). Phycoerythrin-conjugated anti-human CCR2 (hCCR2) mAb 48607 (called αCCR2 in this paper) was obtained from R&D Systems, Inc. (Minneapolis, MN). CCR5 mAb CTC5, fluorescein-labeled CCR5 mAb 3A9, and 2D7 were obtained from BD Pharmingen (San Diego, CA).

Generation of mouse anti-human CCR5 mAbs. Female BALB/c mice were given a primary intraperitoneal immunization with 10^7 CCR5-expressing cells (CHO-CCR5 or L1.2-CCR5) with complete Freund's adjuvant. The second immunization was similarly performed 4 to 6 weeks later except that incomplete Freund's adjuvant was used with the cells. The mice were then boosted at 4- to 6-week intervals with 10^7 CHO-CCR5 or L1.2-CCR5 cells in phosphate-buffered saline (PBS) with no adjuvant. The last immunization was carried out intraperitoneally with 10^7 CCR5-expressing cells or intravenously with 2×10^6 CCR5-expressing cells on the third day before fusion. The spleen cells of the immunized mice were fused with myeloma cells according to methods described previously by Galfré and Milstein (17). Ten days after fusion, the supernatants were tested for specific antibody production by a cell-based enzyme-linked immunosorbent assay (ELISA). Hybridomas that produced the most potent supernatants, as monitored in the CCR5-dependent cell-cell fusion (CCF) assay, were then cloned by limiting dilution or fluorescence-activated cell sorting (FACS). The mAbs were individually purified to >95% homogeneity by protein A chromatography. All mAbs were stored at 4°C in PBS.

Expression plasmid. The human CCR5 receptor open reading frame was subcloned using PCR from TrueClone (catalog no. TC110858; OriGene Technologies, Rockville, MD). The following PCR primers were used in the reaction: 5′ primer 5′-ATA-TAT-TAA-TCT-AGA-ACC-ATG-GAT-TAT-CAA-GTGTCA-AGT-C-3′ and 3′ primer 5′-ATA-TAT-TCT-AGA-GCG-GAT-CCT-CAC-AAG-CCC-ACA-GAT-ATT-TC-3′. The 1.1-kb PCR product was digested with XbaI and BamHI and cloned into the mammalian expression vector pcDNA3.1(−) (Invitrogen, Carlsbad, CA). The sequences of the clones were confirmed and found to contain the identical human CCR5 coding sequence (GenBank accession no. NM_000579). Human CCR2B was cloned from an existing cell line expressing the human CCR2B receptor (catalog no. BACC1; Amersham Biosciences, Piscataway, NJ). The CCR2B coding sequence was amplified from genomic DNA extracted from this cell line by using PCR with the following primer pair: 5′-CATGCTGTCCACATCTCGTTCTCGG-3′ and 5′-TAAACCAGCCGAGA CTTCCTGCTCC-3′. The amplified CCR2B DNA was cloned into the pcDNA3.1/V5-His-TOPO vector (Invitrogen, Carlsbad, CA), and the sequence was verified to be identical to the previously published human CCR2B sequence (GenBank accession no. NM_000648).

CCR5/CCR2B chimeras and CCR5 mutants. In order to generate CCR5/CCR2B chimeras, the extracellular domain of CCR5 or CCR2B was swapped between the two receptors, one at a time. The N-terminal 14-amino-acid sequence was considered to be the N-terminal domain. ECL2 was divided into two domains, ECL2A (Arg168 to Cys178) and ECL2B (Ser179 to Lys197). Some of the CCR5/CCR2B chimeras (CCR5-based CCR5/CCR2B chimeras 25555, 52555, 55255, 55525, and 55552 and CCR2B-based chimera 52222) used to generate data in this study are depicted in Fig. 1. Domain swapping was carried out by using the QuikChange site-directed mutagenesis kit (Stratagene, La Jolla, CA) according to the manufacturer's instructions. The pcDNA3-CCR5 expression plasmid was used as a PCR template for CCR5-based chimeras, and the pcDNA3-CCR2B expression plasmid was used as a PCR template for the CCR2B-based chimeras. The primer pairs used for the generation of the various chimeras are listed in Table 1. Various N-terminal truncated CCR5 expression plasmids (with the first 4, 8, 12, or 20 amino acid residues deleted) were constructed by PCR cloning using the same downstream primer ending at the stop codon and various upstream primers starting at the corresponding positions. Single-amino-acid mutations in CCR5 were generated by using the QuikChange site-directed mutagenesis kit (Stratagene, La Jolla, CA) according to the manufacturer's instructions. All mutations have been sequence verified. All chimeras and CCR5 mutants were transfected into CHO-G16α cells, and stable clones were used for epitope mapping. For stable transfection, CHO-G16α cells were plated in F12 medium supplemented with 10% (vol/vol) fetal bovine serum and 200 μg/ml hygromycin and incubated overnight. On the following day, FuGene 6 (Roche Applied Science) transfection reagent was used for the transfection of all expression plasmids according to the manufacturer's instructions. In brief, plasmid DNAs were mixed with FuGene 6 reagent diluted with serum-free medium. Forty-eight hours after transfection, G418 was introduced into the medium to a final concentration of 1 mg/ml. The stable expression population of CCR5 was enriched by several rounds of FACS by using appropriate antibodies. CCR2B-based chimeras were sorted with CCR2 mAb FAB151P or anti-CCR5 mAb 3A9. CCR5-based chimeras and mutants were sorted with CCR5 mAb CTC5 or 2D7.

Cell-based ELISA. Twenty thousand CHO-CCR5 and/or CHO cells per well were seeded into 96-well tissue culture plates and incubated overnight at 37°C. For the screening of hybridomas, supernatants (50 μl/well) or serially diluted 2D7 control antibody was added to CHO-CCR5 and CHO cells in parallel. Plates were incubated at 4°C for 2 h. Cells were fixed in PBS containing 0.05% (vol/vol) glutaraldehyde for 10 min. After washing three times with assay medium, 50 μl per well of horseradish peroxidase (HRP)-conjugated sheep anti-mouse immunoglobulin G (IgG) antibody (GE Healthcare, Piscataway, NJ) diluted 1:2,000 was added to plates. Plates were incubated at room temperature (RT) for 2 h. After extensive washes with PBS, 50 μl per well tetramethylbenzidine substrate (Roche Applied Science, Indianapolis, IN) was added for color development. The reactions were stopped by adding 25 μl of 1 M sulfuric acid to the reaction mixture. Plates were read at 450 to 620 nm on an Envision plate reader (Perkin-Elmer, Shelton, CT).

FACS analysis. Monoclonal antibodies were labeled with Alexa Fluor 488 using Zenon mouse IgG labeling kits from Molecular Probes (catalog no. Z-25102 for mouse IgG2a and Z-25202 for mouse IgG2b; Molecular Probes, Eugene, OR). One hundred microliters of cells (1×10^5 cells) was stained with 1 μg Zenon-labeled antibody. After incubation for 30 min at RT, the cells were washed three times and resuspended in 300 μl FACS assay buffer.

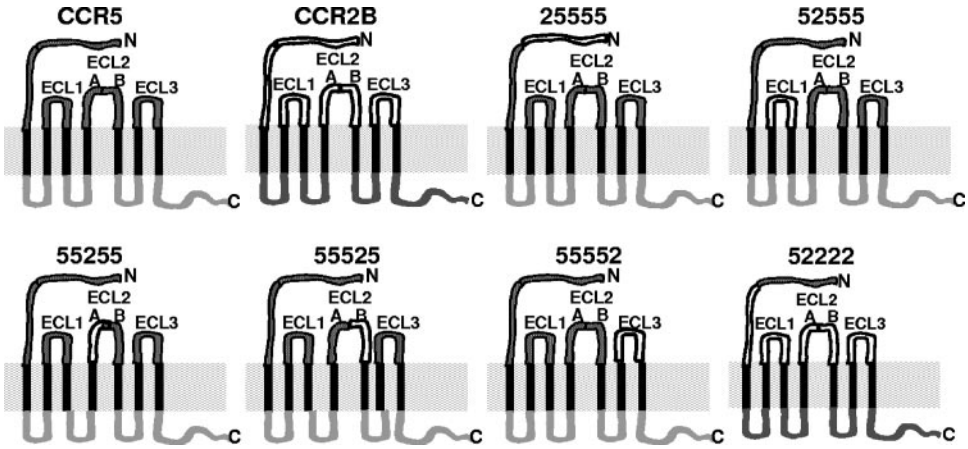

FIG. 1. Schematic diagram of CCR5/CCR2B chimeras. CCR5 and CCR2B molecules both contain seven transmembrane helixes (shown in black), four extracellular domains (N terminus, ECL1, ECL2, and ECL3), and four intracellular domains (intracellular loop 1, 2, and 3 and the C terminus). The largest extracellular loop, ECL2, was divided into ECL2A and ECL2B at Cys178; therefore, there are five extracellular domains depicted in this diagram. For the construction of CCR5/CCR2B chimeras, a single extracellular domain from CCR5 or CCR2B was swapped between the two receptors so that each chimera carries a single extracellular domain from the other receptor. Wild-type CCR5, CCR2B, and various chimeras are indicated on top of each molecule.

The stained cells were analyzed with a FACScan flow cytometer (Becton Dickinson, San Jose, CA).

Epitope mapping. Epitope mapping was performed by using stable cells overexpressing various chimeras or CCR5 mutants by using FACS analysis. To control for variations in the antibody binding signal caused by changes in expression levels for various mutants or chimeras, the CCR5-specific C-terminus-binding mAb C-20 (Santa Cruz Biotechnology, Santa Cruz, CA) was used to stain all CCR5 mutants with cell membrane permeation. Cells were stained with various Alexa-labeled mAbs, and total binding was measured by FACS as described above. The mean fluorescence intensity (MFI) obtained from each mAb was corrected for expression by using the MFI for C-20 as follows: corrected MFI = mAb MFI on CCR5 mutant × (C-20 MFI on CCR5-wild type/C-20 MFI on CCR5 mutant). The percent loss in binding for each mAb was calculated according to the following equation: (1 − corrected mAb MFI/corrected C-20 MFI) × 100%. A positive value indicates a loss in binding and a negative value indicates a gain in binding for a particular mAb and CCR5 mutant. If the changes in binding on a CCR5 mutant were within 20%, this was considered to be insignificant.

TABLE 1. Primers used for the generation of CCR5/CCR2B chimeras

Chimera	Swapped domain[a]	Primer pair
25555	N-terminal aa 1–14 from CCR2B	5′-CGTTTAAACGGGCCCTCTAGAACCATGCTGTCCACATCTCGTTCTC GGTTTATCAGAAATACCTATTATACATCGGAGCCCTGCC-3′ 5′-GGCAGGGCTCCGATGTATAATAGGTATTTCTGATAAACCGAGAAC GAGATGTGGACAGCATGGTTCTAGAGGGCCCGTTTAAACG-3′
52555	ECL1 (aa 89–102)	5′-CCCCTTCTGGGCTCACTCTGCTGCCAACGAGTGGGTCTTTGGAAA TGCAATGTGTAAACTCTTGACAGGGC-3′ 5′-GCCCTGTCAAGAGTTTACACATTGCATTTCCAAAGACCCACTCGTT GGCAGCAGAGTGAGCCCAGAAGGGG-3′
55255	ECL2A (aa 168–178)	5′-CTCCCAGGAATCATCTTTACCAAATGCCAGAAAGAAGATTCTGTT TATGTCTGTAGCTCTCATTTTCCATACAGTC-3′ 5′-GACTGTATGGAAAATGAGAGCTACAGACATAAACAGAATCTTCTT TCTGGCATTTGGTAAAGATGATTCCTGGGAG-3′
55525	ECL2B (aa 179–197)	5′-GAAGGTCTTCATTACACCTGCGGCCCTTATTTTCCACGAGGATGG AATAATTTCCACACAATAATGATAGTCATCTTGGGGCTGGTC-3′ 5′-GACCAGCCCCAAGATGACTATCATTATTGTGTGGAAATTATTCCA TCCTCGTGGAAAATAAGGGCCGCAGGTGTAATGAAGACCTTC-3′
55552	ECL3 (aa 258–280)	5′-CCTTCCAGGAATTCTTTGGCCTGAGTAACTGTGAAAGCACCAGTC AACTGGACCAAGCCACGCAGGTGACAGAGAGACTCTTGG-3′ 5′-CCAAGAGTCTCTGTCACCTGCGTGGCTTGGTCCAGTTGACTGGTG CTTTCACAGTTACTCAGGCCAAAGAATTCCTGGAAGG-3′
52222	N-terminal aa 1–14 from CCR5	5′-GGTGGAATTGCCCTTCATGGATTACCAAGTTAGTTCTCCGATTTAC GACATTAACAACGAGAGCGGTGAAGAAGTCACC-3′ 5′-GACTTCTTCACCGCTCTCGTTGTTAATGTCGTAAATCGGAGAACTA ACTTGGTAATCCATGAAGGGCAATTCCACCAC-3′

[a] aa, amino acids.

CCF assay and antiviral assays. The CCR5-mediated CCF assay was performed as described previously (21). For single-cycle antiviral assays, pseudotyped NL-Bal viruses were produced by cotransfecting 293FT cells (Invitrogen, Carlsbad, CA) with pNL4-3Δenv (HIV pNL4-3 genomic construct with a deletion within the *env* gene) and pcDNA3.1/NL-BAL *env* (pcDNA3.1 plasmid containing the NL-Bal *env* gene [obtained from Roche Welwyn]). The supernatants containing pseudotyped viruses were harvested 2 days following transfection and stored at −80°C in aliquots. Test antibodies were serially diluted in 96-well plates. The equivalent of 1.5×10^5 relative luciferase units of virus stocks and 2.5×10^4 JC53-BL cells were added to each well. Three days later, the Steady-Glo luciferase assay system was added, and luciferase activity was measured by using a luminometer (Luminsokan; Thermo Electron Corporation, Waltham, MA). For antiviral assays in PBMCs, human PBMCs were isolated from buffy coats (obtained from the Stanford Blood Center) by Ficoll-Paque centrifugation. PBMCs (2×10^6 to 4×10^6 cells/ml) were incubated with 2 μg/ml phytohemagglutinin (Invitrogen, Carlsbad, CA) for 24 h at 37°C and then with 5 units/ml human interleukin-2 (Roche Applied Sciences, Indianapolis, IN) for a minimum of 48 h prior to the assay. In a 96-well round-bottom plate, 1×10^5 PBMCs were infected with HIV-1 JR-CSF (kindly provided by Irvin Chen, UCLA) in the presence of serially diluted CCR5 antibody. Plates were incubated for 6 days at 37°C. Virus production was measured at the end of infection by using a p24 ELISA (Perkin-Elmer, Shelton, CT) according to the manufacturer's instructions. For all antiviral assays, the 50% inhibitory concentration (IC_{50}) was calculated by using the sigmoidal dose-response model with one binding site in Microsoft XLFit.

Peptide ELISA. A peptide ELISA was performed as previously described by Khurana et al. (22). Biotinylated 2D7-2SK or 2D7-2SK-K4R (1 μg/well) was captured onto wells coated with 200 ng of streptavidin by incubation at RT for 1.5 h. After blocking with Eagle's minimal essential medium containing 5% (vol/vol) fetal bovine serum, serial dilutions of CCR5 mAbs in blocking solution were added to each well and incubated for 1.5 h at RT. After three washes with PBS containing 0.05% (vol/vol) Tween 20, 50 μl of 1:2,000-diluted HRP-conjugated goat anti-mouse IgG (Bio-Rad, Hercules, CA) was added to each well and incubated for 1 h. The wells were washed three times, and 50 μl of tetramethylbenzidine substrate was added to each well. Color development was stopped by adding 25 μl of 1 M sulfuric acid, and absorbance was measured at 450 nm.

Antibody kinetics studies. CHO-CCR5 cells were used in all kinetics studies, and antibodies bound to cell surface CCR5 were measured by either FACS analysis or fluorescent-linked immunoassay as described below. All experiments were done on ice or at 4°C, and data used in this study were derived from three or more independent experiments. In the kinetics studies, the mAbs were covalently labeled with Alexa 488 by using the Alexa Fluor 488 Microscale Protein Labeling kit (Invitrogen, Carlsbad, CA) according to the manufacturer's instructions. In all FACS assays, an isotype control antibody was used to determine the background, which was subtracted from the MFI values for the test mAbs. For K_d determinations, CHO-CCR5 cells (1×10^5 cells) were incubated with various amounts of labeled mAbs for 45 min. After washing, the cells were subjected to FACS analysis. MFI values were graphed against mAb concentrations using the one-phase exponential associate curves in GraphPad PRIZM software (Intuitive Software for Science, San Diego, CA), and the K_d values were calculated. For on-rate determinations, CHO-CCR5 cells were incubated with 5 μg/ml of each Alexa-labeled mAb for 2, 5, 10, 20, 40, 60, 120, 240, 480, 960, and 1,920 s. At the end of each time point, an equal volume of 2% (vol/vol) formaldehyde was added to the cells to stop binding reactions. Cells were washed three times and subjected to FACS analysis. Data were fit to the one-phase exponential association equation in PRIZM, and the on rate was calculated and expressed as the $T_{0.5on}$ (time required to reach 50% maximal binding). For the determination of off rates, a fluorescent-linked immunoassay was used instead of FACS. CHO-CCR5 cells were plated into 96-well culture plates at 2×10^4 cells per well. On the following day, the cells were fixed in PBS containing 2% (vol/vol) formaldehyde and then incubated with a near-saturation amount of various labeled CCR5 mAbs on ice for 45 min. Following washes, a 15-fold molar excess of the same unlabeled mAb was added to the cells, and the cells were incubated at 4°C for various time periods. At the end of each time point, the cells were washed three times, and the fluorescence signal from the cells was detected by Victor V (Perkin-Elmer, Shelton, CT). The off rate, $T_{0.5off}$ (the time required for 50% of the receptor-bound mAb to dissociate), was calculated by performing nonlinear regression using the one-phase exponential decay equation in PRIZM.

Linear epitope analysis by Western blot. Briefly, CHO cells stably expressing CCR5 wild type or mutants were lysed in denaturing lysis buffer. The clarified cell lysates were run on an 8% sodium dodecyl sulfate-polyacrylamide gel containing 4 M urea equivalent to 2.5×10^5 cells per lane and transferred onto polyvinylidene difluoride membranes. Each blot was stained with 0.5 μg/ml of the novel CCR5 mAbs or CTC5 control mAb (catalog no. MAB1802; R&D Systems, Minneapolis, MN). The primary antibody was detected with secondary HRP-conjugated sheep-anti-mouse IgG antibody (catalog no. NA931V) and ECL Plus Western blotting detection reagents (catalog no. RPN2132) (both from Amersham Biosciences, Piscataway, NJ). The CCR5 signal was visualized by using a Typhoon 9400 system (Amersham Biosciences, Piscataway, NJ).

Homology model of hCCR5. A three-dimensional model of the human CCR5 receptor was constructed on the basis of manual sequence alignments between bovine rhodopsin (31) and the human CCR5 sequence. Using the Protein Modeling tool within Molecular Operating Environment (Chemical Computing Group Inc., Montreal, Canada), the homology model was created from these alignments using the bovine rhodopsin crystal structure as the backbone template for the transmembrane helices. The loop regions that are structurally close to the rhodopsin template were added to the helices by searching a library of protein structures generated from the Protein Data Bank (PDB) (4). The side chain conformations were chosen from a rotamer library (7) and were further refined by energy minimization using a CHARMM22 force field. After obtaining the structure of CCR5 from rhodopsin, both disulfide links were manually inserted between Cys20-Cys269 and Cys101-Cys178. The primary intention of this study was to understand antibody binding to wild-type CCR5 and the loss of binding when certain residues in ECL2 were mutated. Hence, the focus was to obtain a refined structure of the extracellular loops. For this reason, in the molecular dynamic study, helices I to VII and the intracellular loops were restrained to simplify the system. The final three-dimensional structure of the CCR5 receptor was obtained after a set of constrained dynamics and minimization to remove any structural constraints. This CCR5 model consisted of seven transmembrane helical domains connected by three ECLs and three intracellular loops.

RESULTS

Novel CCR5 mAbs with potent antiviral activities. CHO and CHO-CCR5 cell-based ELISAs were developed and described in Materials and Methods. The specificity and sensitivity of the cell-based ELISAs were demonstrated by testing a commercial CCR5 mAb, 2D7. 2D7 specifically binds to CHO-CCR5 cells but not CHO parental cells. This CHO-CCR5-based ELISA system was able to detect 2D7 at concentrations as low as 500 picograms (data not shown). About 26,400 hybridoma lines were screened for CCR5-specific monoclonal antibody production, and about 400 positive clones were identified by using the cell-based ELISA. These positive clones were then screened for antiviral activity by using the CCF assay, a virus-free cell-based surrogate antiviral assay. Seven mAb clones that showed inhibitory effects in the CCF assay were identified. These hybridoma lines were cloned, and the purified mAbs were retested in the CCF assay. All of them were confirmed to be active in CCF, single-cycle antiviral, and PBMC antiviral assays (Table 2). Therefore, these mAb clones were active against three different R5 HIV strains tested: 92US715 (used in the CCF assay), NL-Bal (used in the single-cycle assay), and JR-CSF (used in the PBMC assay). Furthermore, all mAbs showed higher potency in the PBMC antiviral assay than in the CCF and single-cycle antiviral assays. The reason for this is not completely understood. One possible explanation is that the PBMCs express very low levels of CCR5 and that the reporter cells used in the CCF assay overexpress CCR5. It has been shown that HIV infection in cells expressing low-level CCR5 is more susceptible to entry inhibitors (32). Another explanation could be that multiple rounds of HIV infection occur in the PBMC antiviral assay, while a single round of infection/fusion happens in the single-cycle or CCF assay. It is likely that a further reduction of viral production occurs after each additional round of the infection cycle in the presence of CCR5 inhibitors; thus, greater final inhibitory effects may be achieved

TABLE 2. Antiviral activities of CCR5 mAbs[a]

Assay	Avg IC_{50} (μg/ml) ± SD							
	2D7	ROAb10	ROAb13	ROAb18	ROAb14	ROAb12	ROAb36	ROAb51
CCF	0.73 ± 0.18	1.62 ± 0.54	2.10 ± 0.67	0.33 ± 0.13	0.20 ± 0.07	0.51 ± 0.14	23.6 ± 5.29	0.86 ± 0.20
Single-cycle antiviral	1.7 ± 0.57	1.74 ± 0.64	4.33 ± 1.7	0.17 ± 0.03	0.16 ± 0.04	0.18 ± 0.04	17.2 ± 4.37	0.73 ± 0.17
PBMC antiviral	0.34 ± 0.08	0.52 ± 0.12	0.03 ± 0.03	0.02 ± 0.01	0.02 ± 0.02	0.04 ± 0.03	4.6 ± 0.77	0.29 ± 0.09

[a] Data are averages and standard errors from two or more independent experiments.

in the PBMC antiviral assays. Four of the mAbs, ROAb12, ROAb13, ROAb14, and ROAb18, that showed the highest potency in inhibiting HIV replication in PBMCs (IC_{50} = 0.02 to 0.04 μg/ml) were characterized further.

Epitope mapping of novel CCR5 mAbs using CCR5/CCR2B chimeras. CCR5 contains four major extracellular domains: the N-terminal end, ECL1, ECL2, and ECL3. ECL2 is the largest ECL and can be divided into two portions at the highly conserved Cys178. mAbs recognizing ECL2A (N-terminal region) or ECL2B (C-terminal region) have been described previously (25). For the identification of the extracellular domains to which these potent murine mAbs bind, a series of CCR5-based CCR5/CCR2B chimeras was created (Fig. 1). In each chimera, a single extracellular domain on CCR5 was swapped with the counterpart from CCR2B. CCR2B was used to provide the domain substitutes because it is the closest β-chemokine receptor to CCR5, and this may minimize the domain-swapping effect on the overall conformation and surface expression. As shown in Table 3, the four CCR5 mAbs, ROAb12, ROAb13, ROAb14, and ROAb18, that showed the most potent antiviral activities in the PBMC antiviral assays (Table 2) were tested on all CCR5-based chimeras along with control mAb 2D7, whose binding site has been previously mapped to ECL2A (25). Swapping of ECL2A (chimera 55255) completely abolished the binding of 2D7 to CCR5. This also resulted in about 70 to 80% loss of binding of mAbs ROAb12, ROAb14, and ROAb18. Swapping of the ECL2B domain (chimera 55525) also significantly reduced the binding activities of these three mAbs and 2D7. Swapping of other CCR5 extracellular domains did not cause noticeable changes in binding activities for ROAb12, ROAb14, ROAb18, and 2D7. The other mAb, ROAb13, however, bound to wild-type CCR5 and all chimeras except 25555. ROAb13 lost 92% of its binding to CCR5 when the N-terminal end was replaced with that from CCR2B. These results suggest that ROAb13 possibly binds to the Nt of CCR5 and that the other three novel mAbs probably bind to ECL2A and ECL2B (Table 3). To define the binding sites of these mAbs, CCR5 mutants carrying N-terminal truncation and single-amino-acid mutations were utilized.

ROAb13 recognizes the N terminus of CCR5. A series of Nt-truncated CCR5 molecules was used to locate the binding sites of ROAb13. When the N-terminal four residues were truncated, ROAb13 binding to CCR5 lost 42% of its binding activity. The truncation of the N-terminal 8 or 12 residues abolished the binding of ROAb13 to CCR5 (Table 3). This result verified the chimera data showing that ROAb13 binds to the Nt of CCR5. In order to demonstrate that the Nt of CCR5 can be recognized independently of the CCR5 scaffold, the CCR2B Nt was replaced with the CCR5 Nt, and this chimera, 52222, was recognized by ROAb13 but not by other CCR5 mAbs (Fig. 2A). Although this chimera did not express on the CHO cell surface as efficiently as wild-type CCR2B or CCR5, the binding signal to 52222 by ROAb13 was comparable to that

TABLE 3. Normalized CCR5 mAb binding by FACS[a]

Mutant	% Binding				
	2D7	ROAb12	ROAb13	ROAb14	ROAb18
25555	97	106	8	107	98
52555	104	103	95	97	102
55255	0	20	93	21	29
55525	64	62	97	63	69
55552	103	94	102	99	97
CCR5dN4	97	99	58	96	101
CCR5dN8	98	103	0	98	97
CCR5dN12	94	101	0	100	99
Y3A	101	97	74	99	102
S6A	100	96	79	104	97
S7A	99	94	76	103	96
I9A	104	103	59	101	98
K171A	0	11	98	21	11
E172A	0	9	101	21	10
W190A	10	16	103	24	21

[a] Data are averages of two or more independent experiments.

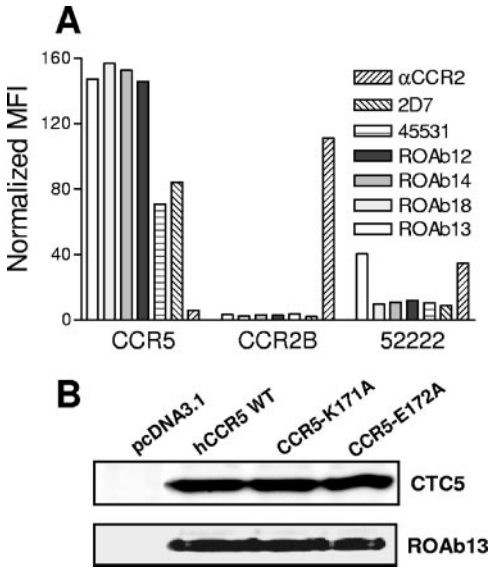

FIG. 2. ROAb13 recognizes linear epitopes in the Nt. (A) FACS analysis. Bars are normalized MFIs for each mAb. (B) Western blot of denatured wild-type (WT) and mutant CCR5 by ROAb13 and the positive control mAb CTC5.

seen with the CCR2B-specific mAb αCCR2, suggesting strong binding by ROAb13 to the CCR5 Nt. To define the residues required for ROAb13 binding, alanine-scanning mutants were generated for the N-terminal 11 residues. As shown in Table 3, none of the single-residue mutations abolished ROAb13 binding. However, mutation Y3A, S6A, S7A, or I9A reduced ROAb13 binding by 21 to 41%, and the rest of the single-residue mutations caused less than 20% changes in ROAb13 binding activity. This result suggests that ROAb13 likely binds to more than one residue at the Nt of CCR5. Previously published data suggested that the majority of CCR5 mAbs recognize conformational epitopes, only a small number of CCR5 mAbs recognize linear epitopes, and almost all of them are Nt-binding antibodies. To determine whether these novel mAbs recognize linear epitopes, denatured CCR5 was detected by these novel mAbs in Western blots. ROAb13 and CTC5 (Nt-binding CCR5 mAbs that have been previously shown to recognize linear epitopes) (25) were found to be able to recognize wild-type CCR5 and the two CCR5 mutants carrying single-residue mutations in ECL2A (Fig. 2B). None of the other three mAbs, ROAb12, ROAb14, and ROAb18, bound to denatured CCR5 (data not shown), suggesting that they recognize conformational epitopes on CCR5.

ROAb12, ROAb14, and ROAb18 recognize ECL2. As described above, ROAb12, ROAb14, and ROAb18 significantly lost their binding to CCR5/CCR2B chimeras 55255 and 55525, suggesting that ECL2A and ECL2B are required for the binding of these three mAbs (Table 3). The control antibody 2D7 also binds to this exodomain. To identify the key residues that are required for the binding of these mAbs, a series of alanine-scanning mutants carrying mutations in ECL1, ECL2, and ECL3 were generated. As shown in Table 3, two mutations in ECL2A (K171A and E172A) completely abolished the binding of 2D7 and reduced the binding of ROAb12, ROAb14, and ROAb18 by 79 to 91%. In contrast, these two mutations did not affect the binding of ROAb13 that recognizes the Nt. These results are in agreement with previously published data, which showed that K171 and E172 are essential for 2D7 binding (25, 30). A single mutation in ECL2B (W190A) also significantly reduced the binding of 2D7, ROAb12, ROAb14, and ROAb18 (90, 84, 76, and 79%, respectively), but it did not change ROAb13 binding (Table 3). None of the other single-amino-acid mutations in ECL2 or some other selected single-amino-acid mutations, D2A, Q4A, P8A, T11A (Nt), D95A (ECL1), E262A, F263A, and F264A (ECL3), caused significant changes in CCR5 binding by any of these mAbs. Thus, the dominant epitopes for these mAbs include K171, E172, and W190.

Epitope-mapping data suggest that ROAb12, ROAb14, and ROAb18 bind to similar epitopes as 2D7. However, functional and binding data suggested that these three novel mAbs are different from 2D7. ROAb12, ROAb14, and ROAb18 demonstrated about 10-fold higher antiviral activity than 2D7 (Table 2); moreover, these mAbs showed binding properties superior to those of 2D7 (see Fig. 5). Although epitope-mapping data indicate that they bind to similar conformational epitopes that reside mainly in ECL2, subtle differences between the epitopes for 2D7 and the three novel mAbs must exist. It has been reported that 2D7 binds with high affinity to a peptide, termed 2D7-2SK, that was identified from a phage display library (22).

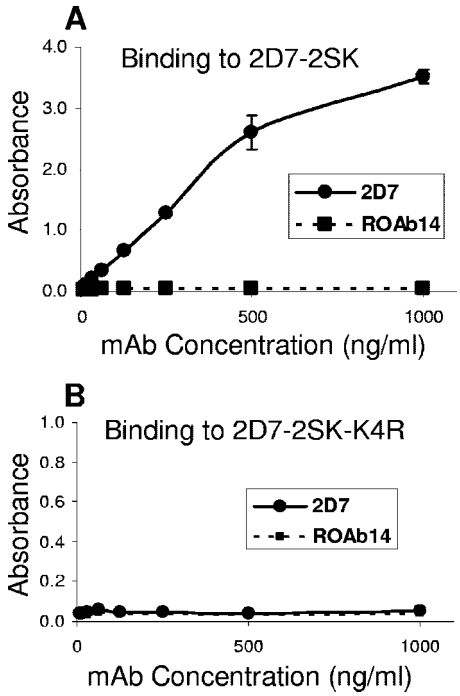

FIG. 3. Peptide ELISA. Antibodies 2D7 and ROAb14 were tested for their binding to peptide 2D7-2SK (A) and its mutated version, 2D7-2SK-K4R (B), in ELISAs. 2D7 binds to peptide 2D7-2SK but not 2D7-2SK-K4R, and ROAb14 does not bind to either peptide.

This peptide contains a sequence that is homologous to two distal regions of CCR5 ECL2 including the Q170-L174 sequence. A mutation of the fourth amino acid, Lys, to Arg in peptide 2D7-2SK (named 2D7-2SK-K4R) abolished the binding of 2D7 to this peptide (22). In the current study, we examined whether mAbs ROAb12, ROAb14, and ROAb18 recognize the linear peptide 2D7-2SK. As shown in Fig. 3, 2D7 binds to peptide 2D7-2SK with high affinity, but it failed to bind to peptide 2D7-2SK-K4R, suggesting that 2D7 binding is highly specific (22). However, mAbs ROAb12, ROAb14, and ROAb18 showed no binding to peptide 2D7-2SK (only ROAb14 is shown). These results suggest that ROAb12, ROAb14, and ROAb18 recognize epitopes that are similar but not identical to those of 2D7.

The dominant epitopes are conserved among different species. Monkey CCR5 shares a high (98%) amino acid sequence identity with human CCR5, and only one amino acid residue differs within ECL2 between monkey and human CCR5 (Fig. 4A). Lysine at position 171 in human CCR5 is replaced by arginine in monkey CCR5. Lys171 is critical for 2D7 binding, and a mutation of Lys171 to alanine results in a complete loss of 2D7 binding. Previously published data suggest that 2D7 does not bind to monkey CCR5, possibly due to the replacement of Lys171 with arginine (38); this is further supported by mutation studies of 2D7 linear epitopes (22). Since Lys171 is also required for the binding of CCR5 by ROAb12, ROAb14, and ROAb18, it would be interesting to find out whether these novel mAbs recognize monkey CCR5. The total binding of Alexa-labeled CCR5 mAbs to CHO cells overexpressing human or monkey CCR5 was monitored by FACS. mAb 2D7, which binds to human CCR5 with high affinity, was unable to

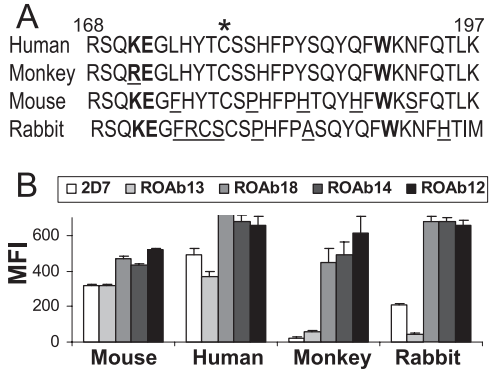

FIG. 4. Novel CCR5 mAbs bind to CCR5 from multiple species. (A) Alignment of human, monkey, rabbit, and mouse CCR5 ECL2 sequences. The GenBank accession numbers for human, monkey, rabbit, and mouse CCR5 are P51681, P61814, ABD79048, and P51682, respectively. The conserved residues K171, E172, and W190 that form the epitopes for mAbs ROAb12, ROAb14, and ROAb18 are shown in boldface type. Residues that are different from the human sequence are underlined. The conserved Cys178 that divides ECL2 into ECL2A and ECL2B is indicated by an *. (B) Binding of CCR5 mAbs to human, monkey, rabbit, and mouse CCR5 by FACS analysis.

bind to monkey CCR5. However, all three novel mAbs, ROAb12, ROAb14, and ROAb18, bind to monkey CCR5 with high affinity, and the K_d values of these three mAbs for monkey and human CCR5 are almost identical. In contrast, ROAb13 showed about a 10-fold lower affinity for monkey CCR5 than for human CCR5 (Table 4). The binding of these mAbs to rabbit and mouse CCR5 was also examined. Rabbit CCR5 and mouse CCR5 share 80% and 81% amino acid sequence identity with human CCR5, respectively, and the dominant epitopes K171, E172, and W190 are conserved. All these four mAbs bind to rabbit CCR5 with high affinity and bind to mouse CCR5 with lower affinity (Table 4). Interestingly, although K171, E172, and W190 are also conserved in dog and rat CCR5, none of the CCR5 mAbs described here recognize them (data not shown), suggesting that dog and rat CCR5 may not possess the conformation to present the epitopes containing these residues correctly on the surface.

It has been observed that 2D7 yielded a higher MFI than many other CCR5 mAbs tested in the same experiment, thus suggesting that 2D7 recognizes a large proportion of cell surface CCR5 (25). In the current study, the four novel mAbs were directly compared with 2D7 in binding to CCR5 of different species using saturating amounts of each mAb. As shown in Fig. 4B, 2D7 exhibited a high saturation MFI (490) in binding to human CCR5. mAb ROAb13 showed a slightly lower MFI than 2D7, and mAbs ROAb12, ROAb14, and ROAb18 yielded the highest MFI (655 to 719) in binding to human CCR5. The latter three mAbs also bind to large proportions of monkey CCR5. mAb 2D7, however, did not show any binding to monkey CCR5. ROAb13, which recognizes the Nt of CCR5, exhibited a very low MFI, consistent with its much lower affinity for monkey CCR5. This is likely due to the significant sequence differences in the N termini of human and monkey CCR5. It is striking that the three novel mAbs ROAb12, ROAb14, and ROAb18 exhibited the highest MFI in binding to CCR5 from all four species, human, monkey, rabbit, and mouse, suggesting that their shared epitope(s) is highly conserved.

ROAb12, ROAb14, and ROAb18 demonstrate favorable binding kinetics. As described above, the four novel CCR5 mAbs ROAb12, ROAb13, ROAb14, and ROAb18 demonstrated highly potent activity in the PBMC antiviral assay by comparison to the control CCR5 mAb 2D7. To investigate whether antiviral potency is associated with binding properties, binding kinetics experiments were performed. mAbs ROAb12, ROAb14, and ROAb18 showed the highest binding affinity for human CCR5, with a K_d range of 0.2 to 0.36 μg/ml. 2D7 and ROAb13 exhibited relatively lower binding affinities for human CCR5, with K_d values of 0.68 and 1.84 μg/ml, respectively (Fig. 5A and D). Interestingly, the K_d values correlate well with the antiviral IC_{50} values for these mAbs. The association and dissociation rates of these mAbs were also determined. All four novel mAbs showed similar $T_{0.5on}$ values (20 to 44 s), which are faster than that of 2D7 (263 s). mAb 2D7 reached binding equilibrium in about 15 min, while the other mAbs reached equilibrium within 5 min (Fig. 5B). In addition, all mAbs exhibited very slow dissociation from CCR5. More than half of the receptors were still occupied by the mAbs even after 20 h of dissociation. The slowest dissociation was observed for the most potent mAbs, ROAb12, ROAb14, and ROAb18, followed by ROAb13 and 2D7 (Fig. 5C). These results suggest that when delivered in vivo as drugs, these novel mAbs may occupy cell surface CCR5 for long periods, thus providing prolonged blockage of CCR5-dependent HIV entry.

ECL2 contains dominant epitopes for potent mAbs. As described above, out of the seven mAbs identified from hybridoma screening, the four mAbs that showed highest potency in the PBMC antiviral assays were further characterized by epitope mapping. Three of them (ROAb12, ROAb14, and ROAb18) recognize the same conformational epitopes located in ECL2, while the fourth mAb, ROAb13, recognizes a linear epitope located at the Nt. To verify the hypothesis that ECL2 has the dominant epitopes for potent CCR5 mAbs, the binding sites for the other three mAbs were also investigated. In order to indirectly obtain information on which domain(s) these

TABLE 4. CCR5 mAbs recognize CCR5 of multiple species[a]

CCR5 species	CCR5 mAb K_d ± SE (μg/ml)				
	2D7	ROAb18	ROAb14	ROAb12	ROAb13
Human	0.68 ± 0.1	0.2 ± 0.018	0.36 ± 0.028	0.28 ± 0.024	1.84 ± 2.13
Monkey	>30	0.31 ± 0.03	0.16 ± 0.02	0.33 ± 0.05	15.9 ± 1.62
Mouse	28.3 ± 5.5	9.7 ± 1.37	10.98 ± 1.35	10.1 ± 1.1	17.0 ± 2.21
Rabbit	1.77 ± 0.31	0.51 ± 0.11	0.52 ± 0.17	0.23 ± 0.09	11.2 ± 0.26

[a] Data are from three or more independent experiments.

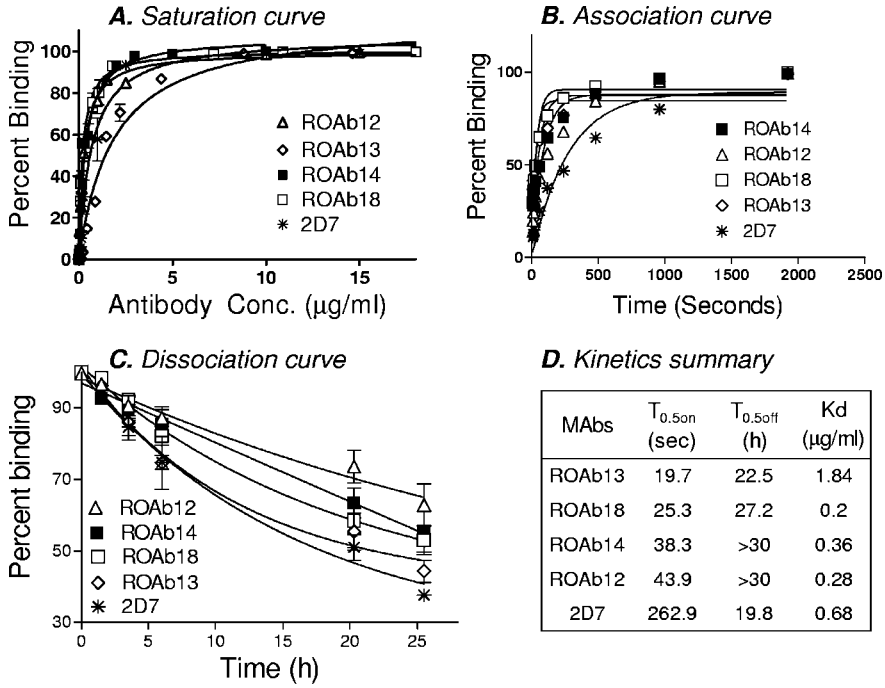

MAbs	$T_{0.5on}$ (sec)	$T_{0.5off}$ (h)	Kd (μg/ml)
ROAb13	19.7	22.5	1.84
ROAb18	25.3	27.2	0.2
ROAb14	38.3	>30	0.36
ROAb12	43.9	>30	0.28
2D7	262.9	19.8	0.68

FIG. 5. Binding kinetics of CCR5 mAbs. (A) Saturation binding curves. (B) Association rate determination. (C) Dissociation rate determination. (D) Summary of K_d, on-rate, and off-rate values for CCR5 mAbs. Results are from three or more independent experiments.

mAbs bind to, binding competition experiments were performed. As shown in Fig. 6A, ROAb10 and ROAb51 strongly inhibited ROAb14 and 2D7 binding, suggesting that they may also bind to ECL2 of CCR5. mAb ROAb36 did not significantly compete for binding with ROAb14, but it weakly competed with 2D7 and strongly competed with ROAb13. These results suggest that ROAb36 most likely binds to the Nt of CCR5, and its binding may interfere with 2D7 binding to some extent. In summary, the two mAbs ROAb10 and ROAb51 that compete with ROAb14 and 2D7 for binding also showed potent antiviral activities; mAb ROAb36, which recognizes epitopes outside of ECL2 regions, showed weak antiviral activity (Table 2).

To further characterize the binding epitopes of these three mAbs, chimeras 25555, 55255, and 55525 were used to determine if any of these mAbs recognize epitopes derived from the Nt or ECL2. As shown in Fig. 6B, mAb ROAb36 showed only 27% binding to chimera 25555 in comparison to wild-type CCR5, suggesting that it most likely recognizes epitopes that reside in the Nt. The other two mAbs, ROAb10 and ROAb51, lost binding to chimera 55255 noticeably (67% and 75%, respectively). These two mAbs bind to the other two chimeras, 25555 and 55525, with slightly lower affinity than that for wild-type CCR5. All three mAbs were also tested for binding to K171A/E172A and W190A mutants. It was found that K171A/E172A mutations markedly reduced the binding of ROAb10 and ROAb51 (87% and 96%, respectively) but not ROAb36. the W190A mutation, however, did not alter the binding of any of the three mAbs to CCR5. Taken together, these results suggest that mAb ROAb36 recognizes the Nt, while ROAb10 and ROAb51 recognize ECL2. Unlike ROAb12, ROAb14,

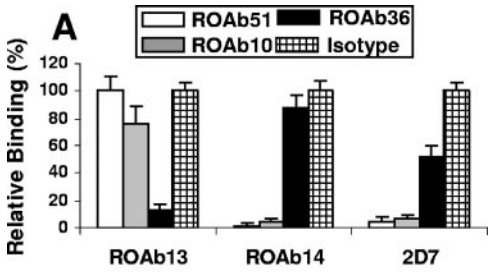

B Normalized binding (%) of CCR5 mAbs

Mutants	ROAb10	ROAb36	ROAb51
25555	76	27	89
55255	33	103	25
55525	75	91	88
K171A/E172A	13	111	4
W190A	96	104	100

FIG. 6. Epitope mapping of additional novel CCR5 mAbs. (A) Binding competition of CCR5 mAbs. CHO-CCR5 cells were incubated with saturating amounts of various CCR5 mAbs (indicated in the box) or the isotype control for 45 min, followed by further incubation with labeled ROAb13, ROAb14, or 2D7 for 30 min. Binding of ROAb13, ROAb14, or 2D7 under competition with various mAbs was measured by FACS, and the relative binding for each competition was calculated by setting the isotype as 100%. (B) CHO cells stably expressing CCR5/CCR2B chimeras 25555, 52555, and 55255 or CCR5 carrying K171A/E172A double mutations or the W190 single mutation were incubated with labeled CCR5 mAb ROAb10, ROAb36, or ROAb51, and relative binding of the mAbs was measured by FACS analysis. The binding of each mAb to the CCR5 chimeras and mutants was normalized against expression levels and expressed as normalized percent binding.

and ROAb18, ROAb10 and ROAb51 require K171 and E172 but not W190.

CCR5 homology model supports the proposed epitopes for ROAb12, ROAb14, and ROAb18. In order to understand the molecular basis for the high affinities and antiviral potencies of mAbs ROAb12, ROAb14, and ROAb18, a three-dimensional homology model of CCR5 was generated by using the rhodopsin structural template (PDB accession no. 1F88). The final homology model of the CCR5 receptor was subjected to constrained minimization and dynamics to study the effect of ECL2 mutations on the conformation of the extracellular loops. The seven transmembrane helices were held fixed during the molecular dynamics study, as our major interest is centered on ECL2. The modeling study clearly identified key residues like W190 and K171 that are required for 2D7, ROAb12, ROAb14, and ROAb18 binding. These residues are exposed to the surface, as shown in Fig. 7A. A shallow pocket can clearly be seen in the center of the CCR5 outer surface, and K171 stands right in the middle of this pocket. This makes a perfect binding site for antibodies.

It is surprising that, according to this model, residue E172 is not exposed to the surface (Fig. 7). This raises a question: how does the E172A mutation influence antibody binding while E172 is buried under the surface? We propose that the loss in binding of these antibodies to CCR5 carrying the E172A mutation is due to conformational changes and dynamic effects of ECL2B. The molecular dynamics study revealed that the conformational changes are due to the space created by the E172A mutant. This concerted conformational change in ECL2 and ECL3 is shown in Fig. 7B. These changes result in the repositioning of F182, thereby allowing a conformational change in K171. The four key residues that move within the binding site are Q170, K171, F182 on ECL2, and Q280 on ECL3. The concerted motion of the residues results in K171 salt bridging with D276 on ECL3. This leads to K171 being buried in the pocket; as a result, it is unable to interact with 2D7, ROAb12, ROAb14, and ROAb18 (Fig. 7B, C, and D).

DISCUSSION

There are four extracellular domains on CCR5 that may potentially serve as antigenic epitopes, and the N-terminal domain is probably the most dominant antigenic site. This domain is the largest extracellular domain, and it is enriched in hydrophilic and aromatic amino acid residues including modified tyrosines. A large number of CCR5 mAbs have been mapped to this domain. Potentially, even more Nt-recognizing mAbs may exist that have not been reported due to the fact that these mAbs are usually weak in binding to CCR5 and blocking viral entry and chemokine binding (25, 30). In this report, among all 400 hybridomas that demonstrated binding to CCR5 by using a cell-based ELISA, less than 10 showed significant activity in inhibiting cell-cell fusion, which were further characterized. Our homology model suggests that the four extracellular domains of CCR5 form the highly organized surface structure with all four domains bridged with two pairs of disulfide bonds. This surface provides multiple conformational epitopes, consistent with the finding that the majority of our characterized CCR5 mAbs recognize conformational epitopes. The mAbs that do recognize linear epitopes are almost all Nt-binding antibodies (25), and this might be explained by the fact that the N-terminal end of CCR5 is the most flexible and the most exposed among all exodomains. While all reported Nt-binding CCR5 mAbs are weak entry inhibitors, ROAb13 demonstrated potent antiviral activities. Like other Nt-recognizing mAbs, ROAb13 is also a weak inhibitor of chemokine-mediated Ca^{2+} flux (30). In fact, ROAb13 is inactive in blocking chemokine-mediated Ca^{2+} flux and cell migration at concentrations of up to 20 μg/ml (data not shown). This unique feature of ROAb13 makes it particularly attractive as an antiviral agent since it spares chemokine function. There have been reports suggesting that a blockade of CCR5 natural function may potentially increase the risk of West Nile virus infection and exacerbate West Nile virus and other microbial infections or inflammatory disease, possibly due to an impaired activation or trafficking of natural killer cells and/or $CD8^+$ cells to sites of infection (1, 3, 10, 18, 19, 29).

Although the coreceptor function of CCR5 requires multiple regions in the exodomain and is conformationally highly complex, it appears that ECL2 is essential (36). Natural antibodies purified from human serum or breast milk using a cyclopeptide mimicking the conformational CCR5 ECL2 demonstrated antiviral effects (5, 6). In addition, sera from monkeys immunized with this ECL2 peptide showed potent antiviral effects. Markedly attenuated acute-phase infection was also observed in these immunized macaques (28). These results suggest that CCR5 ECL2 may contain important epitopes for antibodies with potent antiviral activities.

A large number of CCR5 mAbs that bind to various regions of CCR5 extracellular domains have been reported (25, 30, 43). A majority of the mAbs against CCR5 recognize conformational epitopes derived from one or more extracellular domains (25). Although many CCR5 mAbs have been reported, few of them are potent HIV entry inhibitors (30). These data suggest that certain unique epitopes have to be recognized in order for an antibody to be an effective inhibitor of viral entry. Based on available published information, mAbs recognizing the CCR5 Nt displayed strong inhibition upon gp120 binding to CCR5 but moderate inhibition upon HIV entry; in contrast, mAbs recognizing exclusively or primarily ECL2 are potent HIV entry blockers yet weak or only moderate gp120 binding inhibitors (25, 30, 43). The binding sites for 2D7 and PRO 140 have been mapped to ECL2 and multidomains including ECL2, respectively (25, 30). The recognition sites for PRO 140 comprise Asp2 in the Nt and Arg168 and Tyr176 in ECL2. Both 2D7 and PRO 140 are potent HIV entry inhibitors.

The ECL2-recognizing mAbs can be divided into three classes based on the regions from where their epitopes derive. mAbs in the first class bind exclusively to ECL2A. 2D7 is the first such antibody reported whose epitope has been mapped to K171/E172. The novel mAbs ROAb10 and ROAb51 also fall into this class. A few mAbs can be classified into the second class, which recognize epitopes in ECL2B (mainly from Tyr184 to Phe189) (25). The third class of mAbs recognize epitopes derived primarily from ECL2A but also from ECL2B or other domains. mAb PRO 140 falls into this class, because it requires Arg168 in ECL2A and Asp2 in the Nt (30). The novel mAbs ROAb12, ROAb14, and ROAb18 described here also belong to this class. These three mAbs use epitopes from both ECL2A and ECL2B. The third class of mAbs exhibited the most potent

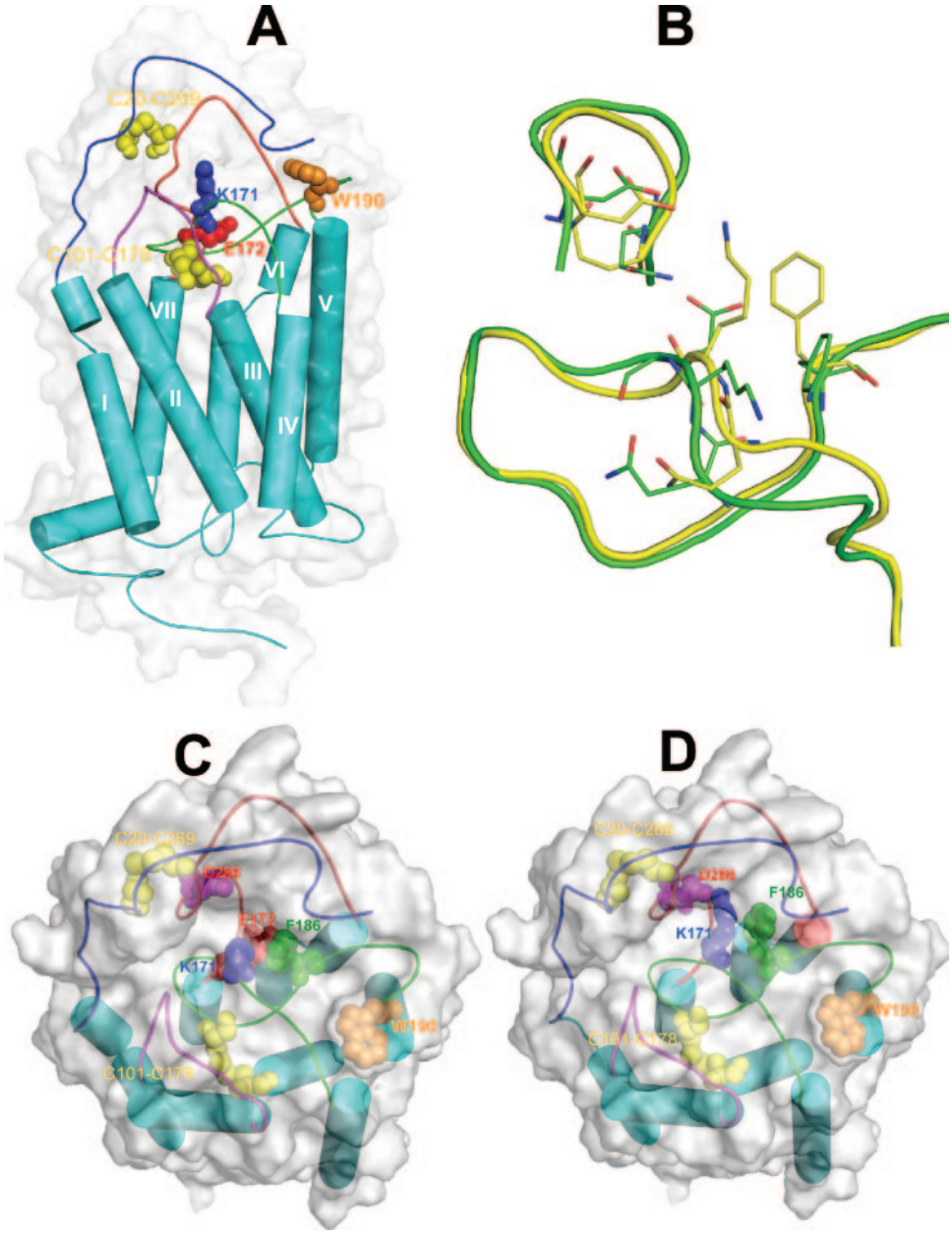

FIG. 7. CCR5 homology modeling. (A) The seven transmembrane helices are marked and shown as cylinders. The N terminus is blue, and ECL1, ECL2, and ECL3 are magenta, green, and red, respectively. The disulfide links between C20-C269 and C101-C178 are shown in yellow. The key residues forming the conformational epitopes for mAbs ROAb12, ROAb14, ROAb18, and 2D7 are W190 (orange), K171 (blue) and E172 (red). The transparent white surface indicates the accessibility of both K171 and W190 by the mAbs. Similar color schemes are used for all panels. (B) The conformational changes in ECL2 and ECL3 are shown. ECL2 and ECL3 for the wild-type receptor and E172A mutant are shown in green and yellow, respectively. These conformational changes are caused by the creation of a space due to an E172A mutation and the repositioning of F182, which leads to significant movement of K171. The four key residues that move around the binding site are Q170, K171, F182 on ECL2, and Q280 on ECL3. The concerted motion of the residues causes the formation of a salt bridge between K171 and D276 (on ECL3). As a result, K171 is buried within the pocket surface so that it is no longer available for antibody binding. (C) A top view of the CCR5 receptor is shown to indicate the accessibility of K171 and W190. The presence of a pocket for antibody binding is clearly seen from this view. Residue E172 is buried and hence not available for interaction with the antibodies. Adjacent residues F182 (green) and D286 (magenta) are also marked. (D) Constrained molecular dynamics followed by minimizations reveal that in an E172A mutant CCR5 receptor, the space within the pocket created by the removal of E172 allows F182 to move out. This conformational change allows K171 to interact with D286 (shown below), which makes K171 inaccessible at the surface for antibody binding. Therefore, we hypothesize that the loss of antibody binding to CCR5 carrying an E172A mutation is an indirect effect involving conformational changes.

antiviral activities, followed by the first class. These data suggest that ECL2A provides the crucial components of the epitopes for CCR5 mAbs with highly potent antiviral activities.

It is intriguing that ROAb12, ROAb14, and ROAb18 bind to monkey CCR5 with high affinity, while 2D7 showed no binding (Fig. 4). The possible reason for this is that an Arg residue is present in monkey CCR5 at position 171 instead of Lys. Although both residues are basic and have similar struc-

tures (Arg is slightly longer than Lys), apparently, 2D7 can recognize Lys only. This result suggests that if Lys171 is part of the epitope for 2D7, the interaction between Lys and the contact sites in the variable region of 2D7 must be highly stringent. In contrast, interactions between Lys171 and mAbs ROAb12, ROAb14, and ROAb18 are more forgiving: they bind to Lys as well as to Arg. There are four to eight acidic residues in the heavy-chain complementarity determining regions of mAbs ROAb12, ROAb14, ROAb18, and 2D7. It is possible that one of these acidic residues may be involved in a direct interaction with Lys171.

G-protein-coupled receptors possess multiple domains and exist in multiple conformational states (40). The different levels of MFI under saturating, equilibrium binding conditions are probably caused by multiple conformational states of CCR5. mAbs with higher MFIs recognize a greater proportion of cell surface CCR5 and vice versa. Previously published data suggest that 2D7 binds to a larger proportion of CCR5 than most other mAbs (25). The three novel mAbs ROAb12, ROAb14, and ROAb18 bind to an even greater proportion of cell surface CCR5 than 2D7, and they also demonstrated higher antiviral potency. These data suggest that the epitopes for these mAbs are dominant epitopes that are present in the majority of cell surface CCR5 molecules. In order to completely inhibit viral infection, not only do the mAbs have to be able to cover all the functional CCR5 molecules but their binding affinity to CCR5 also has to be high enough. As suggested by the homology model of CCR5, K171 and E172 are located in the center of the CCR5 outer surface and form a shallow pocket (Fig. 7). This pocket forms a perfect binding site for antibodies. mAb 2D7 and five out of the six potent novel mAbs described in this paper (ROAb12, ROAb14, ROAb18, ROAb10, and ROAb51) all bind to this pocket. Because this recessed central area may also be critical for interactions with HIV gp120 and chemokines (23, 35), this explains the potent antiviral activities of these mAbs.

mAb drugs have both advantages and disadvantages compared to traditional small-molecule drugs. mAbs can be dosed infrequently (biweekly or even monthly), they have less off-target toxicity due to their high specificity, and they usually do not interfere with small-molecule drugs and are thus suitable for combination with any small-molecule drugs. The main disadvantage of antibody drugs is that they have to be administered by injection. In addition, mAb drugs are generally less cost-effective than small-molecule drugs, and they may cause potential immunotoxicity.

In summary, by screening over 26,000 hybridomas, we found about 400 clones that showed specific binding to CCR5 as demonstrated by cell-based ELISA. However, out of these 400 clones, only 7 showed anti-HIV activity. Furthermore, only six mAb clones showed antiviral potency equal to or better than that of the control mAb 2D7, sufficient for being clinical drug candidates. Out of these six mAbs, except for one mAb, ROAb13, which recognizes a linear epitope residing in the Nt of CCR5, all other five mAbs recognize epitopes derived from ECL2. Besides, the control mAb 2D7, which is in preclinical development as an HIV entry inhibitor, also recognizes a similar epitope in ECL2. In addition, two out of three key residues (Arg168 and Tyr176) that are required for binding by the highly potent CCR5 mAb PRO 140 are located in ECL2. Therefore, based on these data, we hypothesize that CCR5 ECL2 contains the dominant epitopes for potent anti-HIV mAbs.

ACKNOWLEDGMENTS

We acknowledge our colleagues Lisa Zautke, Jekle Andreas, and Gabrielle Heilek-Snyder at Roche Palo Alto for providing the single-cycle and PBMC antiviral data used in this paper. We also thank Irvin Chen for providing the JR-CSF virus and Julian Symons at Roche Palo Alto for his critical comments on the manuscript.

REFERENCES

1. **Ank, N., K. Petersen, L. Malmgaard, S. C. Mogensen, and S. R. Paludan.** 2005. Age-dependent role for CCR5 in antiviral host defense against herpes simplex virus type 2. J. Virol. **79:**9831–9841.
2. **Baritaki, S., A. Zafiropoulos, M. Sioumpara, M. Politis, D. A. Spandidos, and E. Krambovitis.** 2002. Ionic interaction of the HIV-1 V3 domain with CCR5 and deregulation of T lymphocyte function. Biochem. Biophys. Res. Commun. **298:**574–580.
3. **Barr, E. L., S. Ouburg, J. U. Igietseme, S. A. Morre, E. Okwandu, F. O. Eko, G. Ifere, T. Belay, Q. He, D. Lyn, G. Nwankwo, J. Lillard, C. M. Black, and G. A. Ananaba.** 2005. Host inflammatory response and development of complications of Chlamydia trachomatis genital infection in CCR5-deficient mice and subfertile women with the CCR5delta32 gene deletion. J. Microbiol. Immunol. Infect. **38:**244–254.
4. **Bernstein, F. C., T. F. Koetzle, G. J. Williams, E. F. Meyer, Jr., M. D. Brice, J. R. Rodgers, O. Kennard, T. Shimanouchi, and M. Tasumi.** 1977. The Protein Data Bank: a computer-based archival file for macromolecular structures. J. Mol. Biol. **112:**535–542.
5. **Bouhlal, H., H. Hocini, C. Quillent-Gregoire, V. Donkova, S. Rose, A. Amara, R. Longhi, N. Haeffner-Cavaillon, A. Beretta, S. V. Kaveri, and M. D. Kazatchkine.** 2001. Antibodies to C-C chemokine receptor 5 in normal human IgG block infection of macrophages and lymphocytes with primary R5-tropic strains of HIV-1. J. Immunol. **166:**7606–7611.
6. **Bouhlal, H., V. Latry, M. Requena, S. Aubry, S. V. Kaveri, M. D. Kazatchkine, L. Belec, and H. Hocini.** 2005. Natural antibodies to CCR5 from breast milk block infection of macrophages and dendritic cells with primary R5-tropic HIV-1. J. Immunol. **174:**7202–7209.
7. **Bower, M. J., F. E. Cohen, and R. L. Dunbrack, Jr.** 1997. Prediction of protein side-chain rotamers from a backbone-dependent rotamer library: a new homology modeling tool. J. Mol. Biol. **267:**1268–1282.
8. **Cocchi, F., A. L. DeVico, A. Garzino-Demo, A. Cara, R. C. Gallo, and P. Lusso.** 1996. The V3 domain of the HIV-1 gp120 envelope glycoprotein is critical for chemokine-mediated blockade of infection. Nat. Med. **2:**1244–1247.
9. **Cormier, E. G., D. N. Tran, L. Yukhayeva, W. C. Olson, and T. Dragic.** 2001. Mapping the determinants of the CCR5 amino-terminal sulfopeptide interaction with soluble human immunodeficiency virus type 1 gp120-CD4 complexes. J. Virol. **75:**5541–5549.
10. **de Lemos, C., J. E. Christensen, A. Nansen, T. Moos, B. Lu, C. Gerard, J. P. Christensen, and A. R. Thomsen.** 2005. Opposing effects of CXCR3 and CCR5 deficiency on CD8+ T cell-mediated inflammation in the central nervous system of virus-infected mice. J. Immunol. **175:**1767–1775.
11. **Deng, H., R. Liu, W. Ellmeier, S. Choe, D. Unutmaz, M. Burkhart, P. Di Marzio, S. Marmon, R. E. Sutton, C. M. Hill, C. B. Davis, S. C. Peiper, T. J. Schall, D. R. Littman, and N. R. Landau.** 1996. Identification of a major co-receptor for primary isolates of HIV-1. Nature **381:**661–666.
12. **Dragic, T., V. Litwin, G. P. Allaway, S. R. Martin, Y. Huang, K. A. Nagashima, C. Cayanan, P. J. Maddon, R. A. Koup, J. P. Moore, and W. A. Paxton.** 1996. HIV-1 entry into CD4+ cells is mediated by the chemokine receptor CC-CKR-5. Nature **381:**667–673.
13. **Dragic, T., A. Trkola, D. A. Thompson, E. G. Cormier, F. A. Kajumo, E. Maxwell, S. W. Lin, W. Ying, S. O. Smith, T. P. Sakmar, and J. P. Moore.** 2000. A binding pocket for a small molecule inhibitor of HIV-1 entry within the transmembrane helices of CCR5. Proc. Natl. Acad. Sci. USA **97:**5639–5644.
14. **Eugen-Olsen, J., A. K. Iversen, P. Garred, U. Koppelhus, C. Pedersen, T. L. Benfield, A. M. Sorensen, T. Katzenstein, E. Dickmeiss, J. Gerstoft, P. Skinhoj, A. Svejgaard, J. O. Nielsen, and B. Hofmann.** 1997. Heterozygosity for a deletion in the CKR-5 gene leads to prolonged AIDS-free survival and slower CD4 T-cell decline in a cohort of HIV-seropositive individuals. AIDS **11:**305–310.
15. **Farzan, M., T. Mirzabekov, P. Kolchinsky, R. Wyatt, M. Cayabyab, N. P. Gerard, C. Gerard, J. Sodroski, and H. Choe.** 1999. Tyrosine sulfation of the amino terminus of CCR5 facilitates HIV-1 entry. Cell **96:**667–676.
16. **Feng, Y., C. C. Broder, P. E. Kennedy, and E. A. Berger.** 1996. HIV-1 entry cofactor: functional cDNA cloning of a seven-transmembrane, G protein-coupled receptor. Science **272:**872–877.

17. **Galfré, G., and C. Milstein.** 1981. Preparation of monoclonal antibodies: strategies and procedures. Methods Enzymol. **73:**3–46.
18. **Glass, W. G., J. K. Lim, R. Cholera, A. G. Pletnev, J. L. Gao, and P. M. Murphy.** 2005. Chemokine receptor CCR5 promotes leukocyte trafficking to the brain and survival in West Nile virus infection. J. Exp. Med. **202:**1087–1098.
19. **Glass, W. G., D. H. McDermott, J. K. Lim, S. Lekhong, S. F. Yu, W. A. Frank, J. Pape, R. C. Cheshier, and P. M. Murphy.** 2006. CCR5 deficiency increases risk of symptomatic West Nile virus infection. J. Exp. Med. **203:**35–40.
20. **Ji, C., M. Brandt, M. Dioszegi, A. Jekle, S. Schwoerer, S. Challand, J. Zhang, Y. Chen, L. Zautke, G. Achhammer, M. Baehner, S. Kroetz, G. Heilek-Snyder, R. Schumacher, N. Cammack, and S. Sankuratri.** 5 December 2006, posting date. Novel CCR5 monoclonal antibodies with potent and broad-spectrum anti-HIV activities. Antivir. Res. doi:10.1016/j.antiviral. 2006.11.003.
21. **Ji, C., J. Zhang, N. Cammack, and S. Sankuratri.** 2006. Development of a novel dual CCR5-dependent and CXCR4-dependent cell-cell fusion assay system with inducible gp160 expression. J. Biomol. Screen. **11:**65–74.
22. **Khurana, S., M. Kennedy, L. R. King, and H. Golding.** 2005. Identification of a linear peptide recognized by monoclonal antibody 2D7 capable of generating CCR5-specific antibodies with human immunodeficiency virus-neutralizing activity. J. Virol. **79:**6791–6800.
23. **Kuhmann, S. E., E. J. Platt, S. L. Kozak, and D. Kabat.** 1997. Polymorphisms in the CCR5 genes of African green monkeys and mice implicate specific amino acids in infections by simian and human immunodeficiency viruses. J. Virol. **71:**8642–8656.
24. **Lalezari, J., M. Thompson, P. Kumar, P. Piliero, R. Davey, K. Patterson, A. Shachoy-Clark, K. Adkison, J. Demarest, Y. Lou, M. Berrey, and S. Piscitelli.** 2005. Antiviral activity and safety of 873140, a novel CCR5 antagonist, during short-term monotherapy in HIV-infected adults. AIDS **19:**1443–1448.
25. **Lee, B., M. Sharron, C. Blanpain, B. J. Doranz, J. Vakili, P. Setoh, E. Berg, G. Liu, H. R. Guy, S. R. Durell, M. Parmentier, C. N. Chang, K. Price, M. Tsang, and R. W. Doms.** 1999. Epitope mapping of CCR5 reveals multiple conformational states and distinct but overlapping structures involved in chemokine and coreceptor function. J. Biol. Chem. **274:**9617–9626.
26. **Liu, R., W. A. Paxton, S. Choe, D. Ceradini, S. R. Martin, R. Horuk, M. E. MacDonald, H. Stuhlmann, R. A. Koup, and N. R. Landau.** 1996. Homozygous defect in HIV-1 coreceptor accounts for resistance of some multiply-exposed individuals to HIV-1 infection. Cell **86:**367–377.
27. **Maeda, K., H. Nakata, Y. Koh, T. Miyakawa, H. Ogata, Y. Takaoka, S. Shibayama, K. Sagawa, D. Fukushima, J. Moravek, Y. Koyanagi, and H. Mitsuya.** 2004. Spirodiketopiperazine-based CCR5 inhibitor which preserves CC-chemokine/CCR5 interactions and exerts potent activity against R5 human immunodeficiency virus type 1 in vitro. J. Virol. **78:**8654–8662.
28. **Misumi, S., D. Nakayama, M. Kusaba, T. Iiboshi, R. Mukai, K. Tachibana, T. Nakasone, M. Umeda, H. Shibata, M. Endo, N. Takamune, and S. Shoji.** 2006. Effects of immunization with CCR5-based cycloimmunogen on simian/HIVSF162P3 challenge. J. Immunol. **176:**463–471.
29. **Moreno, C., T. Gustot, C. Nicaise, E. Quertinmont, N. Nagy, M. Parmentier, O. Le Moine, J. Deviere, and H. Louis.** 2005. CCR5 deficiency exacerbates T-cell-mediated hepatitis in mice. Hepatology **42:**854–862.
30. **Olson, W. C., G. E. Rabut, K. A. Nagashima, D. N. Tran, D. J. Anselma, S. P. Monard, J. P. Segal, D. A. Thompson, F. Kajumo, Y. Guo, J. P. Moore, P. J. Maddon, and T. Dragic.** 1999. Differential inhibition of human immunodeficiency virus type 1 fusion, gp120 binding, and CC-chemokine activity by monoclonal antibodies to CCR5. J. Virol. **73:**4145–4155.
31. **Palczewski, K., T. Kumasaka, T. Hori, C. A. Behnke, H. Motoshima, B. A. Fox, I. Le Trong, D. C. Teller, T. Okada, R. E. Stenkamp, M. Yamamoto, and M. Miyano.** 2000. Crystal structure of rhodopsin: a G protein-coupled receptor. Science **289:**739–745.
32. **Platt, E. J., J. P. Durnin, and D. Kabat.** 2005. Kinetic factors control efficiencies of cell entry, efficacies of entry inhibitors, and mechanisms of adaptation of human immunodeficiency virus. J. Virol. **79:**4347–4356.
33. **Rabut, G. E., J. A. Konner, F. Kajumo, J. P. Moore, and T. Dragic.** 1998. Alanine substitutions of polar and nonpolar residues in the amino-terminal domain of CCR5 differently impair entry of macrophage- and dualtropic isolates of human immunodeficiency virus type 1. J. Virol. **72:**3464–3468.
34. **Rizzuto, C. D., R. Wyatt, N. Hernandez-Ramos, Y. Sun, P. D. Kwong, W. A. Hendrickson, and J. Sodroski.** 1998. A conserved HIV gp120 glycoprotein structure involved in chemokine receptor binding. Science **280:**1949–1953.
35. **Ross, T. M., P. D. Bieniasz, and B. R. Cullen.** 1998. Multiple residues contribute to the inability of murine CCR-5 to function as a coreceptor for macrophage-tropic human immunodeficiency virus type 1 isolates. J. Virol. **72:**1918–1924.
36. **Rucker, J., M. Samson, B. J. Doranz, F. Libert, J. F. Berson, Y. Yi, R. J. Smyth, R. G. Collman, C. C. Broder, G. Vassart, R. W. Doms, and M. Parmentier.** 1996. Regions in beta-chemokine receptors CCR5 and CCR2b that determine HIV-1 cofactor specificity. Cell **87:**437–446.
37. **Samson, M., F. Libert, B. J. Doranz, J. Rucker, C. Liesnard, C. M. Farber, S. Saragosti, C. Lapoumeroulie, J. Cognaux, C. Forceille, G. Muyldermans, C. Verhofstede, G. Burtonboy, M. Georges, T. Imai, S. Rana, Y. Yi, R. J. Smyth, R. G. Collman, R. W. Doms, G. Vassart, and M. Parmentier.** 1996. Resistance to HIV-1 infection in Caucasian individuals bearing mutant alleles of the CCR-5 chemokine receptor gene. Nature **382:**722–725.
38. **Siciliano, S. J., S. E. Kuhmann, Y. Weng, N. Madani, M. S. Springer, J. E. Lineberger, R. Danzeisen, M. D. Miller, M. P. Kavanaugh, J. A. DeMartino, and D. Kabat.** 1999. A critical site in the core of the CCR5 chemokine receptor required for binding and infectivity of human immunodeficiency virus type 1. J. Biol. Chem. **274:**1905–1913.
39. **Trkola, A., T. J. Ketas, K. A. Nagashima, L. Zhao, T. Cilliers, L. Morris, J. P. Moore, P. J. Maddon, and W. C. Olson.** 2001. Potent, broad-spectrum inhibition of human immunodeficiency virus type 1 by the CCR5 monoclonal antibody PRO 140. J. Virol. **75:**579–588.
40. **Vauquelin, G., and I. Van Liefde.** 2005. G protein-coupled receptors: a count of 1001 conformations. Fundam. Clin. Pharmacol. **19:**45–56.
41. **Watson, C., S. Jenkinson, W. Kazmierski, and T. Kenakin.** 2005. The CCR5 receptor-based mechanism of action of 873140, a potent allosteric noncompetitive HIV entry inhibitor. Mol. Pharmacol. **67:**1268–1282.
42. **Wood, A., and D. Armour.** 2005. The discovery of the CCR5 receptor antagonist, UK-427,857, a new agent for the treatment of HIV infection and AIDS. Prog. Med. Chem. **43:**239–271.
43. **Wu, L., G. LaRosa, N. Kassam, C. J. Gordon, H. Heath, N. Ruffing, H. Chen, J. Humblias, M. Samson, M. Parmentier, J. P. Moore, and C. R. Mackay.** 1997. Interaction of chemokine receptor CCR5 with its ligands: multiple domains for HIV-1 gp120 binding and a single domain for chemokine binding. J. Exp. Med. **186:**1373–1381.